11

Four-bar linkages

11.1 *Introduction*

A four bar linkage consists of four rigid bodies, which are called bars or links. The rigid bodies are attached to each other by joints or pivots to form a closed kinematic loop. Four bar linkages are used to perform a wide variety of motions, with just a few movable parts.

11.2 *Basic linkage concepts*

Linkages of practical interest are

1. *revolute* — 1 degree of freedom
2. *prismatic* — 1 degree of freedom
3. *cylindrical* — 2 degrees of freedom
4. *spherical* — 3 degrees of freedom

A four bar linkage can be characterized by its number of degrees of freedom, or its *mobility*, M. This quantity can be shown to be a function of the connectivity, joint degrees of freedom (or mobility), and the overall freedom of the mechanism (i.e., 2D or 3D) through Grübler's equation:

$$M = \lambda(l - j - 1) + \sum_{i=1}^{j} f_i, \tag{11.1}$$

where l is the number of links, j is the number of joints, f_i is the number of degrees of freedom of joint i, and λ is an integer: 3 for plane, spherical, or some spatial linkages, and 6 for most other spatial linkages.

Example 11.2.1. Planar linkages mostly have only one degree of freedom, i.e.,

$$\begin{aligned} M &= 3l - 3j - 3 + j = 1 \\ 2j - 3l + 4 &= 0 \end{aligned} .$$

For a four-bar linkage where $l = 4$ and $j = 4$, we obtain $M = 3 \cdot 4 - 3 \cdot 4 - 3 + 4 = 12 - 12 - 3 + 4 = 1$.

11.3 *Analytical design*

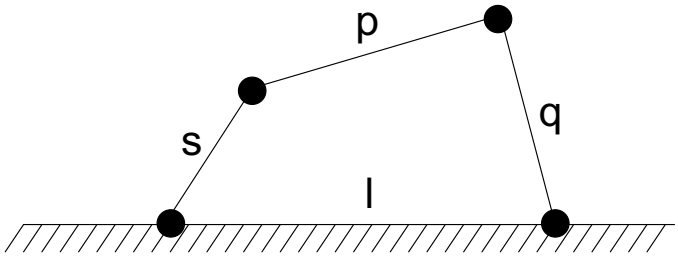

Figure 11.1: Typical four-bar linkage.

The inequality 5-1 is Grashof's criterion. *Grashof's criterion*, or the *mobility criterion* determines whether rotation through 360° is possible or not. If the longest link in a typical linkage (Fig. 11.1) is denoted by l, and the shortest by s, then at least one of the three mobile links can rotate through 360° if $l + s \leq p + q$. When a linkage rotates 360° it is called a *crank*, when it does not, it is called a *rocker*. Combinations are possible, so for example if in Fig. 11.1 link s rotates through 360° at left while the right link q does not, the motion is called a *crank-rocker* motion.

If the longest and shortest link is larger than the sum of the lengths p and q, a so-called *rocker/rocker* motion occurs. In other words, if $l + s > p + q$, all three mobile links will rock and cannot rotate all the way around.

To derive the equations of motion of a four bar linkage, we treat the linkages as vectors. Once the equations of motion are derived, numerical techniques can be used to find the position and velocity of all joints as a function of time. Considering the links to be vectors, one can write

$$l_1 + l_2 + l_3 + l_4 = 0. \tag{11.2}$$

Projection on the x-axis provides

$$l_2 \cos\theta_2 + l_3 \cos\theta_3 - l_4 \cos\theta_4 - l_1 = 0, \tag{11.3}$$

and projection on the y-axis results in

$$l_2 \sin\theta_2 + l_3 \sin\theta_3 - l_4 \sin\theta_4 = 0. \tag{11.4}$$

The angle θ_2 is the given input, i.e., it is the driven joint (e.g., by an electrical motor). Hence, eqns. (11.3) and (11.4) are two nonlinear equations with two unknowns (θ_3, θ_4). Unfortunately these equations are transcendental in terms of the unknowns, and so direct solution is not possible. Two possible solution methods are presented in this course reader:

- The iterative approach, also called the *Freudenstein solution*: Combine both equations, guess either θ_3 or θ_4, solve for the values of θ_3 and θ_4, and then use this new result as the new guess to repeat until either the correct solution is found or the process diverges (at which point the other method must be used).
- Two-dimensional root finder via Newton-Raphson method (recall we mentioned this for nonlinear problems on page 117). This method always works, but is relatively complicated.

11.4 *Iterative approach (Freudenstein)*

Starting from eqn. (11.3), one finds after squaring both sides and rearranging both sides of the equation

$$l_3^2 \cos^2\theta_3 = (l_1 + l_4\cos\theta_4 - l_2\cos\theta_2)^2 = \\ l_1^2 + l_4^2\cos^2\theta_4 + l_2^2\cos^2\theta_2 + 2l_1l_4\cos\theta_4 - 2l_1l_2\cos\theta_2 - 2l_4l_2\cos\theta_4\cos\theta_2. \tag{11.5}$$

Equivalently, from eqn. (11.4), one may find

$$l_3^2 \sin^2\theta_3 = l_4^2\sin^2\theta_4 + l_2^2\sin^2\theta_2 - 2l_2l_4\sin\theta_4\sin\theta_2. \tag{11.6}$$

Adding eqns. (11.5) and (11.6) gives

$$l_3^2 = l_1^2 + l_4^2 + l_2^2 + 2l_1l_4\cos\theta_4 - 2l_1l_2\cos\theta_2 - 2l_2l_4\left(\cos\theta_4\cos\theta_2 + \sin\theta_4\sin\theta_2\right). \tag{11.7}$$

Equation (11.7) reduces to

$$l_3^2 = l_1^2 + l_4^2 + l_2^2 + 2l_1(l_4\cos\theta_4 - l_2\cos\theta_2) - 2l_2l_4\cos(\theta_2 - \theta_4). \tag{11.8}$$

To facilitate the calculations, the following dimensionless parameters are used:

$$L_1 = \frac{l_1}{l_4}, L_2 = \frac{l_1}{l_2}, L_3 = \frac{l_2^2 - l_3^2 + l_4^2 + l_1^2}{2l_2l_4}. \tag{11.9}$$

Introducing the dimensionless parameters from eqn. (11.9) into eqn. (11.8), one obtains

$$L_3 - \cos(\theta_2 - \theta_4) + L_2\cos\theta_4 - L_1\cos\theta_2 = 0. \tag{11.10}$$

Equation (11.10) is called the *Freudenstein equation for a 4-bar linkage*. In eqn. (11.10), the design parameters are θ_2, L_1, L_2, and L_3. One must determine θ_4, the output angle. An iterative solution to equation (11.10) can be obtained by rewriting it as follows

$$L_2 \cos\theta_4 = L_1 \cos\theta_2 - L_3 + \cos(\theta_2 - \theta_4). \tag{11.11}$$

In eqn. (11.11), the unknown angle θ_4 occurs on the left hand side as well as on the right hand side of the equation. To find a solution for eqn. (11.11), one assumes an approximate value of θ_4 (initial guess) in the first iteration. This initial guess can be obtained from a sketch of the linkage. One can substitute this initial guess for θ_4 in the right hand side of eqn. (11.11) to obtain an improved solution for θ_4. Denoting the improved value by index $k+1$ and the original value by index k, one can write

$$\theta_4^{k+1} = \cos^{-1}\frac{1}{L_2}\left\{L_1 \cos\theta_2 - L_3 + \cos(\theta_2 - \theta_4^k)\right\} \tag{11.12}$$

where $k = 1, 2, 3, 4, \ldots$.

The iteration continues until the absolute value of the difference between the current and the improved value for θ_4 is smaller than a predefined convergence criterion ε. The convergence criterion can be chosen according to the desired accuracy of the solution, i.e., the solution will be more accurate for smaller ε:

$$\left|\theta_4^{k+1} - \theta_4^k\right| < \varepsilon. \tag{11.13}$$

In general, it is reasonable to assume that an angle has to be determined with an accuracy of 0.1 degrees, corresponding to $\theta = 0.1\,\frac{2\pi}{360} = 0.00175$ radians.

11.5 *Two-dimensional root finder (Newton-Raphson)*

The simple iteration scheme discussed above does not always converge, and a two-dimensional iterative scheme must then be applied. The two dimensional scheme is an extension of the one dimensional Newton-Raphson method.

11.5.1 *One-dimensional Newton-Raphson method*

The one dimensional *Newton-Raphson method* can be used to find the root of the one dimensional equation $f = y(x)$, i.e., $f(p) = 0$, where $x = p$ is a single root. We assume that $y = f(x)$ can be expanded in a Taylor series around x_0, the initial guess. The initial guess x_0 is in the vicinity of the root, i.e., $|x_0 - p|$ is "small". Expanding $y = f(x)$ as a Taylor expansion at point x_0 gives

$$f(x) = f(x_0) + f'(x_0)(x - x_0) + f''(x_0)\frac{(x - x_0)^2}{2} + \ldots \tag{11.14}$$

or,

$$f(p) = 0 = f(x_0) + f'(x_0)(p - x_0) + f''(x_0)\frac{(p - x_0)^2}{2} + \dots \quad (11.15)$$

If x_0 is close to the root, one can approximate eqn. (11.15) as

$$0 \cong f(x_0) + f'(x_0)(p - x_0) \quad (11.16)$$

and thus

$$p \approx x_0 - \frac{f(x_0)}{f'(x_0)} \quad (11.17)$$

which should be a better approximation to p than x_0. The Newton-Raphson algorithm can then be expressed as

$$p_{n+1} = p_n - \frac{f(p_n)}{f'(p_n)}. \quad (11.18)$$

11.5.2 *Two-dimensional Newton-Raphson method*

The two-dimensional Newton-Raphson follows the same approach as the one-dimensional approach. However, the method deals with two simultaneous equations with two variables:

$$f_1(x,y) = 0 \qquad \text{and} \qquad f_2(x,y) = 0. \quad (11.19)$$

Both are continuous and differentiable and may be written in a Taylor series expansion:

$$\begin{aligned} f_1(x_{i+1},y_{i+1}) &= f_1(x_i,y_i) + \frac{\partial f_1}{\partial x}(x_{i+1} - x_i) + \frac{\partial f_1}{\partial y}(y_{i+1} - y_i) + \dots \text{H.O.T.} \\ f_2(x_{i+1},y_{i+1}) &= f_2(x_i,y_i) + \frac{\partial f_2}{\partial x}(x_{i+1} - x_i) + \frac{\partial f_2}{\partial y}(y_{i+1} - y_i) + \dots \text{H.O.T.}, \end{aligned} \quad (11.20)$$

where H.O.T. denotes higher order terms. We assume x_{i+1}, y_{i+1} are close to the actual root and that $f_1(x_{i+1}, y_{i+1})$ and $f_2(x_{i+1}, y_{i+1})$ are close to zero. Thus, the higher order terms and the left hand sides of eqns. (11.20) can be neglected. This results in

$$\begin{aligned} 0 &= f_1(x_i,y_i) + \frac{\partial f_1}{\partial x}(x_{i+1} - x_i) + \frac{\partial f_1}{\partial y}(y_{i+1} - y_i) \\ 0 &= f_2(x_i,y_i) + \frac{\partial f_2}{\partial x}(x_{i+1} - x_i) + \frac{\partial f_2}{\partial y}(y_{i+1} - y_i). \end{aligned} \quad (11.21)$$

To simplify the notation, one can introduce

$$x_{i+1} - x_i = h \qquad \text{and} \qquad y_{i+1} - y_i = k. \quad (11.22)$$

Substituting eqns. (11.22) into eqns. (11.21), one finds

$$\begin{aligned} 0 &= f_1(x_i,y_i) + \frac{\partial f_1}{\partial x}h + \frac{\partial f_1}{\partial y}k \\ 0 &= f_2(x_i,y_i) + \frac{\partial f_2}{\partial x}h + \frac{\partial f_2}{\partial y}k. \end{aligned} \quad (11.23)$$

This can be rearranged as

$$\begin{aligned} r_1 &= -f_1(x_i, y_i) = \frac{\partial f_1}{\partial x} h + \frac{\partial f_1}{\partial y} k \\ r_2 &= -f_2(x_i, y_i) = \frac{\partial f_2}{\partial x} h + \frac{\partial f_2}{\partial y} k. \end{aligned} \tag{11.24}$$

Here, r_1 and r_2 are called the *residuals*. The solution of eqns. (11.24) can be found with Cramer's method, i.e.,

$$h = \frac{\begin{vmatrix} (-f_1(x_i, y_i)) \left(\frac{\partial f_1}{\partial y}\right) \\ (-f_2(x_i, y_i)) \left(\frac{\partial f_2}{\partial y}\right) \end{vmatrix}}{\begin{vmatrix} \frac{\partial f_1}{\partial x} & \frac{\partial f_1}{\partial y} \\ \frac{\partial f_2}{\partial x} & \frac{\partial f_2}{\partial y} \end{vmatrix}} \tag{11.25}$$

and

$$k = \frac{\begin{vmatrix} \left(\frac{\partial f_1}{\partial x}\right) (-f_1(x_i, y_i)) \\ \left(\frac{\partial f_2}{\partial x}\right) (-f_2(x_i, y_i)) \end{vmatrix}}{\begin{vmatrix} \frac{\partial f_1}{\partial x} & \frac{\partial f_1}{\partial y} \\ \frac{\partial f_2}{\partial x} & \frac{\partial f_2}{\partial y} \end{vmatrix}}. \tag{11.26}$$

Equations (11.25) and (11.26) can be rewritten as

$$h = \frac{1}{A} \left(r_1 \frac{\partial f_2}{\partial y} - r_2 \frac{\partial f_1}{\partial y} \right) \tag{11.27}$$

$$k = \frac{1}{A} \left(r_2 \frac{\partial f_1}{\partial x} - r_1 \frac{\partial f_2}{\partial x} \right) \tag{11.28}$$

where

$$A = \frac{\partial f_1}{\partial x} \frac{\partial f_2}{\partial y} - \frac{\partial f_2}{\partial x} \frac{\partial f_1}{\partial y}. \tag{11.29}$$

Substituting eqns. (11.27) and (11.28) into eqns. (11.22) gives an improved solution for x_{i+1} and y_{i+1}. Repeating the previous procedure for x_{i+2}, y_{i+2} assuming x_{i+1} and y_{i+1} are known, results in an improved solution. This procedure is continued until the predefined convergence criterion is satisfied.

The algorithm can be summarized as follows:

- Decide on a convergence criterion ε: $h < \varepsilon$ and $k < \varepsilon$.
- Starting with an initial guess, $x = x_0$,$y = y_0$, calculate the residuals r_1 and r_2 from eqns. (11.24).
- Calculate A from eqn. (11.29).
- Calculate h, k from eqns. (11.27) and (11.28).
- Determine x_{i+1} and y_{i+1} from eqns. (11.22).

- Check whether the convergence criterion in (step 1) is satisfied.
- Continue step 2 through step 6 until the convergence criterion is satisfied.

11.6 *Application of the Newton-Raphson method to a four bar mechanism*

As indicated earlier, θ_3 and θ_4 are the unknowns in the calculation. One wants to determine an improved solution for the unknown angles θ_3 and θ_4 from an initial guess obtained by making a sketch of the linkage. Replacing x and y in eqns. (11.22) by θ_3 and θ_4, one obtains

$$\theta_3^{i+1} = \theta_3^i + h(\theta_3, \theta_4) \tag{11.30}$$

and

$$\theta_4^{i+1} = \theta_4^i + k(\theta_3, \theta_4). \tag{11.31}$$

The residuals r_1 and r_2 can be calculated as

$$r_1 = -f_1(\theta_3, \theta_4) = \frac{\partial f_1}{\partial \theta_3} h + \frac{\partial f_1}{\partial \theta_4} k \tag{11.32}$$

and

$$r_2 = -f_2(\theta_3, \theta_4) = \frac{\partial f_2}{\partial \theta_3} h + \frac{\partial f_2}{\partial \theta_4} k. \tag{11.33}$$

The solution gives

$$h = \frac{1}{A}(r_1 \frac{\partial f_2}{\partial \theta_4} - r_2 \frac{\partial f_1}{\partial \theta_4}) \tag{11.34}$$

and

$$k = \frac{1}{A}(r_2 \frac{\partial f_1}{\partial \theta_3} - r_1 \frac{\partial f_2}{\partial \theta_3}), \tag{11.35}$$

where

$$A = \frac{\partial f_1}{\partial \theta_3} \frac{\partial f_2}{\partial \theta_4} - \frac{\partial f_2}{\partial \theta_3} \frac{\partial f_1}{\partial \theta_4}. \tag{11.36}$$

In order to determine h, k, and A one needs to calculate the partial derivatives $\frac{\partial f_1}{\partial \theta_3}$, $\frac{\partial f_2}{\partial \theta_4}$, $\frac{\partial f_1}{\partial \theta_4}$ and $\frac{\partial f_2}{\partial \theta_3}$.

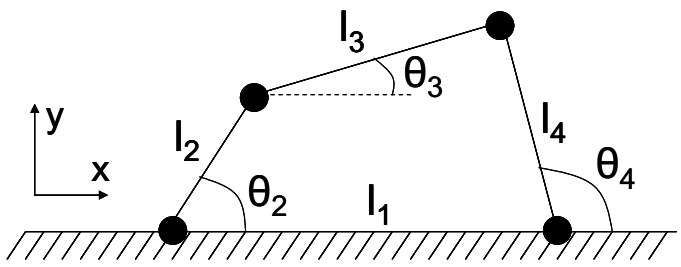

Figure 11.2: Four-bar linkage.

For the linkage shown in Fig. 11.2, the partial derivatives can be calculated from eqns. (11.3) and (11.4):

$$\frac{\partial f_1}{\partial \theta_3} = -l_3 \sin\theta_3 \qquad \frac{\partial f_1}{\partial \theta_4} = l_4 \sin\theta_4 \qquad \frac{\partial f_2}{\partial \theta_3} = l_3 \cos\theta_3 \qquad \frac{\partial f_2}{\partial \theta_4} = -l_4 \cos\theta_4 \tag{11.37}$$

and

$$A = l_3 l_4 \sin\theta_3 \cos\theta_4 - (l_3 \cos\theta_3)(l_4 \sin\theta_4) = l_3 l_4 \sin(\theta_3 - \theta_4). \tag{11.38}$$

Substituting eqns. (11.37) into eqns. (11.34) and (11.35), one obtains

$$\Delta\theta_3 = h(\theta_3, \theta_4) = \frac{-1}{A}(r_1 l_4 \cos\theta_4 + r_2 l_4 \sin\theta_4) = \frac{-l_4}{A}(r_1 \cos\theta_4 + r_2 \sin\theta_4) \tag{11.39}$$

and

$$\Delta\theta_4 = k(\theta_3, \theta_4) = \frac{-1}{A}(r_2 l_3 \sin\theta_3 + r_1 l_3 \cos\theta_3) = \frac{-l_3}{A}(r_2 \sin\theta_3 + r_1 \cos\theta_3). \tag{11.40}$$

After calculating $\Delta\theta_3$ and $\Delta\theta_4$ (h and k), one may obtain an improved solution from eqns. (11.30) and (11.31). The algorithm can be summarized as follows

- Decide on a value of the convergence criterion ϵ that $\Delta\theta_3$ and $\Delta\theta_4$ should not exceed (e.g.$\varepsilon \leq 0.1°$).
- Calculate $-f_1(\theta_3, \theta_4)$ and $-f_2(\theta_3, \theta_4)$ for a chosen initial guess θ_3^i and θ_4^i.
- Evaluate the Jacobian A from eqn. (11.38).
- Determine $\Delta\theta_3$ and $\Delta\theta_4$ from eqns. (11.39) and (11.40).
- The improved solution can then be calculated using eqns. (11.30) and (11.31).
- If $|\Delta\theta_3| < \varepsilon$ and $|\Delta\theta_4| < \varepsilon$, convergence is achieved and the iteration process can be stopped. Else, repeat steps 2 to 5 until convergence is achieved.

11.7 *Calculation of four bar linkage kinematics using polar notation*

11.7.1 *Review of complex polar notation*

The use of complex polar notation allows the calculation of linkage problems in a compact and accurate fashion. In complex polar notation, Euler's equation is

$$e^{i\theta} = \cos\theta + i \sin\theta \tag{11.41}$$

with $i^2 = -1$. Furthermore, vector $\boldsymbol{a}$ is given by

$$\boldsymbol{a} = a e^{i\theta} = a(\cos\theta + i \sin\theta) = a_x + i a_y. \tag{11.42}$$

Note that

$$e^{i\phi}e^{i\theta} = e^{i(\phi+\theta)} = \cos(\phi+\theta) + i\sin(\phi+\theta). \tag{11.43}$$

So a multiplication of $e^{i\phi}$ by $e^{i\theta}$ corresponds to a rotation over an angle θ. Finally, multiplication of $\boldsymbol{a} = ae^{i\theta}$ by $i = \sqrt{-1}$ corresponds to a rotation of $\pi/2$ in the positive (counter-clockwise) sense:

$$i = e^{i\frac{\pi}{2}} = \cos\frac{\pi}{2} + i\sin\frac{\pi}{2} = i, \tag{11.44}$$

$$i\boldsymbol{a} = i \cdot ae^{i\theta} = ia(\cos\theta + i\sin\theta), \tag{11.45}$$

and

$$i\boldsymbol{a} = ae^{i(\theta+\pi/2)}. \tag{11.46}$$

11.7.2 *Application of polar notation to a four bar linkage*

Using complex polar notation, one obtains for the four bar linkage shown in Fig. 11.2 that

$$l_2e^{i\theta_2} + l_3e^{i\theta_3} + l_4e^{i(\pi+\theta_4)} + l_1e^{i\pi} = 0. \tag{11.47}$$

Note that

$$\cos(\pi+\theta_4) = -\cos\theta_4 \qquad \text{and} \qquad \sin(\pi+\theta_4) = -\sin\theta_4. \tag{11.48}$$

Expanding eqn. (11.47) and taking eqns. (11.48) into account, one obtains

$$l_2(\cos\theta_2 + i\sin\theta_2) + l_3(\cos\theta_3 + i\sin\theta_3) + l_4(-\cos\theta_4 - i\sin\theta_4) - l_1 = 0. \tag{11.49}$$

In eqn. (11.49), both the real and the imaginary part of the equation are independently equal to zero. Thus,

$$l_2\cos\theta_2 + l_3\cos\theta_3 - l_4\cos\theta_4 - l_1 = 0 \tag{11.50}$$

and

$$i(l_2\sin\theta_2 + l_3\sin\theta_3 - l_4\sin\theta_4) = 0. \tag{11.51}$$

Equation (11.50) is the projection on the x-axis of the linkage while Equation (11.51) is the projection of the linkage on the y-axis. These equations are identical to the equations for the linkage without using polar notation. The advantage of the polar notation is its compact format. The velocity and acceleration can easily be determined by differentiation.

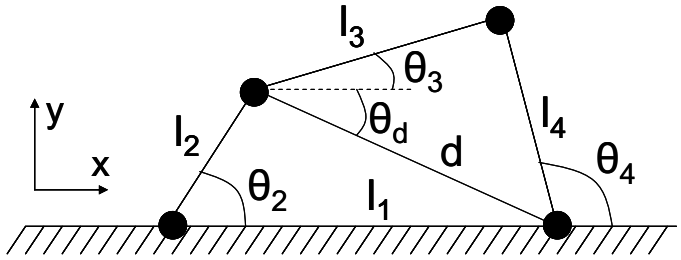

Figure 11.3: Four-bar linkage with polar notation.

11.7.3 *Closed-form solution of a four bar linkage's kinematics with polar notation*

In addition to the iterative solutions discussed above, it is possible to analytically determine the position of a four bar linkage illustrated in Fig. 11.3.

Assume that l_1, l_2, l_3, l_4 and θ_2 are known; d, θ_d, θ_3, and θ_4 can be obtained using the following method:

- Determine d from
$$l_2 e^{i\theta_2} + d e^{i\theta_d} = l_1, \tag{11.52}$$
eliminating θ_d by solving for $d e^{i\theta_d}$, and multiplying each side of the equation by its complex conjugate
$$(d e^{i\theta_d})(d e^{-i\theta_d}) = (l_1 - l_2 e^{i\theta_2})(l_1 - l_2 e^{-i\theta_2}) : \tag{11.53}$$
$$d^2 = l_1^2 + l_2^2 - l_1 l_2 (e^{i\theta_2} + e^{-i\theta_2}) \tag{11.54}$$
and
$$d = (l_1^2 + l_2^2 - 2 l_1 l_2 \cos\theta_2)^{1/2} \tag{11.55}$$
since
$$e^{i\theta} + e^{-i\theta} = 2\cos\theta. \tag{11.56}$$
- Resolve eqn. (11.52) into real and imaginary parts
$$l_2(\cos\theta_2 + i\sin\theta_2) + d(\cos\theta_d + i\sin\theta_d) = l_1. \tag{11.57}$$
Hence,
$$l_2 \cos\theta_2 = l_1 - d\cos\theta_d \tag{11.58}$$
and
$$l_2 \sin\theta_2 = 0 - d\sin\theta_d. \tag{11.59}$$
Then
$$\sin\theta_d = \frac{-l_2}{d}\sin\theta_2, \tag{11.60}$$
$$\cos\theta_d = \frac{l_1 - l_2\cos\theta_2}{d}, \tag{11.61}$$

and

$$\tan\theta_d = \frac{-l_2 \sin\theta_2}{l_1 - l_2\cos\theta_2}. \tag{11.62}$$

- Next, determine the angle θ_3

$$l_3 e^{i\theta_3} = d e^{i\theta_d} + l_4 e^{i\theta_4}. \tag{11.63}$$

Rearranging eqn. (11.63) gives

$$l_3 e^{i\theta_3} - d e^{i\theta_d} = l_4 e^{i\theta_4}. \tag{11.64}$$

Again, multiplying each side of the equation by its complex conjugate gives

$$(l_3 e^{i\theta_3} - d e^{i\theta_d})(l_3 e^{-i\theta_3} - d e^{-i\theta_d}) = l_4 e^{i\theta_4} l_4 e^{-i\theta_4}, \tag{11.65}$$

$$l_3^2 + d^2 - l_3 d(e^{i(\theta_3-\theta_d)} + e^{-i(\theta_3-\theta_d)}) = l_4^2, \tag{11.66}$$

and so

$$l_3^2 + d^2 - l_3 d(2\cos(\theta_3 - \theta_d)) = l_4^2. \tag{11.67}$$

Hence,

$$\cos(\theta_3 - \theta_d) = \frac{l_3^2 + d^2 - l_4^2}{2 l_3 d}. \tag{11.68}$$

- Note that θ_d is known from eqn. (11.62). Now one can determine θ_3 from eqn. (11.68). The output angle θ_4 can found from the complex part of eqn. (11.64):

$$l_3(\sin\theta_3) = d\sin\theta_d + l_4\sin\theta_4. \tag{11.69}$$

- Thus,

$$\sin\theta_4 = \frac{-d\sin\theta_d + l_3\sin\theta_3}{l_4}. \tag{11.70}$$

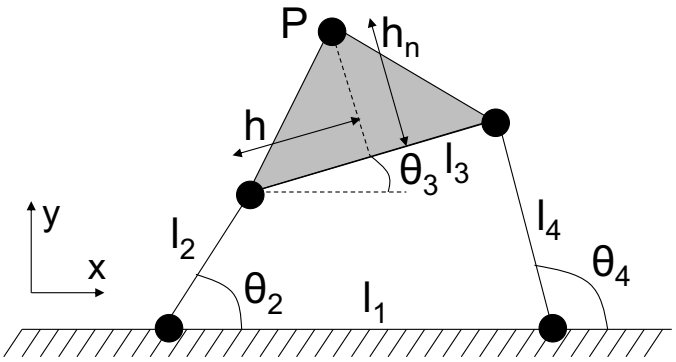

Figure 11.4: Four-bar linkage with coupler body.

11.7.4 *Position of a point on a coupler curve*

If θ_2, θ_3 and θ_4 are given along with l_2, l_3, l_4, h and h_N, then the coordinates of P are given by

$$r_P = l_2 e^{i\theta_2} + h e^{i\theta_3} + h_N e^{i(\theta_3+\frac{\pi}{2})}. \tag{11.71}$$

Expanding eqn. (11.71) gives

$$\begin{aligned} x_p + iy_p &= l_2(\cos\theta_2 + i\sin\theta_2) + h(\cos\theta_3 + i\sin\theta_3) + h_N\left[\cos(\theta_3+\frac{\pi}{2}) + i\sin\left(\theta_3+\frac{\pi}{2}\right)\right] \\ x_p + iy_p &= l_2\cos\theta_2 + h\cos\theta_3 + h_N\cos\left(\theta_3+\frac{\pi}{2}\right) + i\left[l_2\sin\theta_2 + h\sin\theta_3 + h_N\sin\left(\theta_3+\frac{\pi}{2}\right)\right], \end{aligned} \tag{11.72}$$

producing

$$\begin{aligned} x_p &= l_2\cos\theta_2 + h\cos\theta_3 - h_N\sin\theta_3 \\ y_p &= l_2\sin\theta_2 + h\sin\theta_3 + h_N\cos\theta_3 \end{aligned}. \tag{11.73}$$

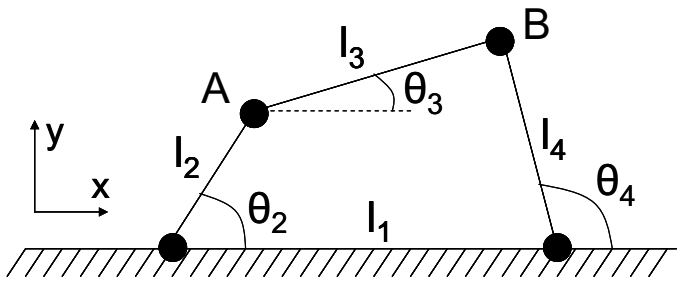

Figure 11.5: Four-bar linkage: determining the velocity of the components.

11.7.5 *Velocity analysis of a four bar linkage*

$$\boldsymbol{l_B} = l_2 e^{i\theta_2} + l_3 e^{i\theta_3} = l_1 + l_4 e^{i\theta_4} \tag{11.74}$$

Differentiating eqn. (11.74) with respect to time gives

$$\frac{d\boldsymbol{l_B}}{dt} = l_2\dot{\theta}_2 i e^{i\theta_2} + l_3\dot{\theta}_3 i e^{i\theta_3} = l_4\dot{\theta}_4 i e^{i\theta_4}. \tag{11.75}$$

Separating real and imaginary parts gives

$$l_2(\cos\theta_2 + i\sin\theta_2)i\dot{\theta}_2 + l_3\dot{\theta}_3 i(\cos\theta_3 + i\sin\theta_3) = l_4\dot{\theta}_4 i(\cos\theta_4 + i\sin\theta_4). \tag{11.76}$$

Thus,

$$\begin{aligned} -l_2\dot{\theta}_2\sin\theta_2 - l_3\dot{\theta}_3\sin\theta_3 &= -l_4\dot{\theta}_4\sin\theta_4 \\ l_2\dot{\theta}_2\cos\theta_2 + l_3\dot{\theta}_3\cos\theta_3 &= l_4\dot{\theta}_4\cos\theta_4. \end{aligned} \tag{11.77}$$

Rearrange eqns. (11.77) with $\dot{\theta}_3$ and $\dot{\theta}_4$ on the left hand side to find

$$\begin{aligned} \dot{\theta}_3(-l_3\sin\theta_3) + \dot{\theta}_4(l_4\sin\theta_4) &= l_2\dot{\theta}_2\sin\theta_2 \\ \dot{\theta}_3(l_3\cos\theta_3) + \dot{\theta}_4(-l_4\cos\theta_4) &= -l_2\dot{\theta}_2\cos\theta_2. \end{aligned} \tag{11.78}$$

In eqns. (11.78), the only unknowns are $\dot{\theta}_3$ and $\dot{\theta}_4$. To obtain the angular velocities $\dot{\theta}_3$ and $\dot{\theta}_4$, the Cramer's method can be used:

$$\dot{\theta}_3 = \frac{\begin{vmatrix} l_2\dot{\theta}_2\sin\theta_2 & l_4\sin\theta_4 \\ -l_2\dot{\theta}_2\cos\theta_2 & -l_4\cos\theta_4 \end{vmatrix}}{\begin{vmatrix} -l_3\sin\theta_3 & l_4\sin\theta_4 \\ l_3\cos\theta_3 & -l_4\cos\theta_4 \end{vmatrix}} \tag{11.79}$$

or, simplifying,

$$\dot{\theta}_3 = \dot{\theta}_2 \frac{-l_2 l_4 \sin\theta_2\cos\theta_4 + l_4 l_2 \sin\theta_4\cos\theta_2}{l_3 l_4 \sin\theta_3\cos\theta_4 - l_4 l_3 \sin\theta_4\cos\theta_3}. \tag{11.80}$$

Finally,

$$\dot{\theta}_3 = \dot{\theta}_2 \frac{l_2}{l_3}\frac{\sin(\theta_4-\theta_2)}{\sin(\theta_3-\theta_4)}. \tag{11.81}$$

Furthermore,

$$\dot{\theta}_4 = \frac{\dot{\theta}_2(l_2 l_3 \sin\theta_3\cos\theta_2 - l_2 l_3\cos\theta_3\sin\theta_2)}{l_3 l_4\sin\theta_3\cos\theta_4 - l_4 l_3\sin\theta_4\cos\theta_3} \tag{11.82}$$

or

$$\dot{\theta}_4 = \dot{\theta}_2 \frac{l_2\sin(\theta_3-\theta_2)}{l_4\sin(\theta_3-\theta_4)}. \tag{11.83}$$

The angular velocities $\dot{\theta}_3$ and $\dot{\theta}_4$ can be obtained if θ_3 and θ_4 are known. The angular velocity $\dot{\theta}_3$ is a function of $\dot{\theta}_2$, $\theta_4-\theta_2$, and $\theta_3-\theta_4$, while the angular velocity $\dot{\theta}_4$ is a function of $\dot{\theta}_2$, $\theta_3-\theta_2$, and $\theta_3-\theta_4$.

A physical interpretation of the velocities in a four bar linkage can be obtained by looking at the velocity equations. From the velocity equation (11.75), we have

$$l_2\dot{\theta}_2 i e^{i\theta_2} + l_3\dot{\theta}_3 i e^{i\theta_3} = l_4\dot{\theta}_4 i e^{i\theta_4},$$

where each term corresponds to a specific velocity:

- First term: Velocity of the crank
- Second term: Velocity of the coupler
- Third term: Velocity of the rocker

This can also be interpreted to mean the motion of point B is the motion of point A plus the relative motion of B around A. One can also determine the velocity of point of a four bar linkage using a graphical method. In the past, when computers were not available, graphical determination of linkages was often required.

The intersection of $\overline{A_0A}$ and $\overline{B_0B}$ gives $P_{b,d}$ which is an "instantaneous rotation axis", or "velocity pole". This means that the motion of AB can be considered instantaneously as a rotation about $P_{b,d}$. Thus, $v_A = \overline{P_{b,a}A}\omega_{b,d}$ and $v_B = \overline{P_{b,a}B}\omega_{b,d}$, where $\omega_{b,d}$ is the instantaneous

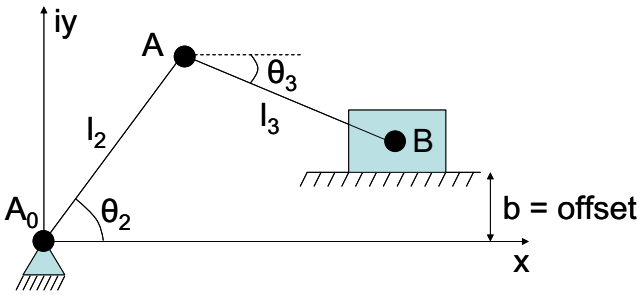

Figure 11.6: Four-bar linkage: the graphical method for determining the velocities.

angular velocity around $P_{b,d}$ and v_A and v_B are the velocities of points A and B, respectively. Eliminating $\omega_{b,d}$ between both velocities gives

$$\frac{v_A}{\overline{P_{b,a}A}} = \frac{v_B}{\overline{P_{b,d}B}}. \tag{11.84}$$

Since $v_A = \omega_A \overline{A_0 A}$, one finds

$$v_B = \overline{A_0 A} \cdot \omega_A \cdot \frac{\overline{P_{b,d}B}}{\overline{P_{b,a}A}}. \tag{11.85}$$

Hence, the measurement of distances $\overline{P_{b,a}A}$ and $\overline{P_{b,d}B}$ with eqn. (11.85) gives v_B.

11.7.6 *Acceleration analysis of a four bar linkage*

Calculating the second derivative of the position of the four bar linkage, expressed by eqn. (11.74), gives

$$\frac{d^2}{dt^2}\left(l_2 e^{i\theta_2} + l_3 e^{i\theta_3}\right) = \frac{d^2}{dt^2}\left(l_1 + l_4 e^{i\theta_4}\right) \tag{11.86}$$

or

$$\frac{d^2 \boldsymbol{l_B}}{dt^2} = l_2 \ddot{\theta}_2 i e^{i\theta_2} + l_2 \dot{\theta}_2^2 (-1) e^{i\theta_2} + l_3 \ddot{\theta}_3 i e^{i\theta_3} - l_3 \dot{\theta}_3^2 e^{i\theta_3}, \tag{11.87}$$

producing

$$\frac{d^2 \boldsymbol{l_B}}{dt^2} = l_4 \ddot{\theta}_4 i e^{i\theta_4} + l_4 \dot{\theta}_4^2 (-1) e^{i\theta_4}. \tag{11.88}$$

Separation of real and imaginary parts gives, respectively,

$$\begin{aligned} l_2 \ddot{\theta}_2 (-1) \sin\theta_2 - l_2 \dot{\theta}_2^2 \cos\theta_2 + l_3 \ddot{\theta}_3 (-1) \sin\theta_3 - l_3 \dot{\theta}_3^2 \cos\theta_3 \\ = l_4 \ddot{\theta}_4 (-1) \sin\theta_4 + l_4 \dot{\theta}_4^2 (-1) \cos\theta_4. \end{aligned} \tag{11.89}$$

$$\begin{aligned} l_2 \ddot{\theta}_2 \cos\theta_2 + l_2 \dot{\theta}_2^2 (-1) \sin\theta_2 + l_3 \ddot{\theta}_3 \cos\theta_3 - l_3 \dot{\theta}_3^2 \sin\theta_3 \\ = l_4 \ddot{\theta}_4 \cos\theta_4 - l_4 \dot{\theta}_4^2 \sin\theta_4 \end{aligned} \tag{11.90}$$

Now one can solve for $\ddot{\theta}_3$ and $\ddot{\theta}_4$:

$$\begin{aligned} \ddot{\theta}_3 (-l_3 \sin\theta_3) + \ddot{\theta}_4 l_4 \sin\theta_4 = \\ l_2 \ddot{\theta}_2 \sin\theta_2 + l_2 \dot{\theta}_2^2 \cos\theta_2 + l_3 \dot{\theta}_3^2 \cos\theta_3 - l_4 \dot{\theta}_4^2 \cos\theta_4 = A \end{aligned} \tag{11.91}$$

$$\begin{aligned}&\ddot{\theta}_3(l_3\cos\theta_3) - \ddot{\theta}_4 l_4\cos\theta_4 = \\ &l_2\ddot{\theta}_2\cos\theta_2 + l_2\dot{\theta}_2^2\sin\theta_2 + l_3\dot{\theta}_3^2\sin\theta_3 - l_4\dot{\theta}_4^2\sin\theta_4 = B\end{aligned}. \tag{11.92}$$

Equations (11.91) and (11.92) can be solved with Cramer's method:

$$\ddot{\theta}_3 = \frac{1}{l_3}\frac{(-A\cos\theta_4 - B\sin\theta_4)}{\sin(\theta_3 - \theta_4)} \tag{11.93}$$

and

$$\ddot{\theta}_4 = \frac{1}{l_4}\frac{(B\sin\theta_3 - A\cos\theta_3)}{\sin(\theta_3 - \theta_4)}. \tag{11.94}$$

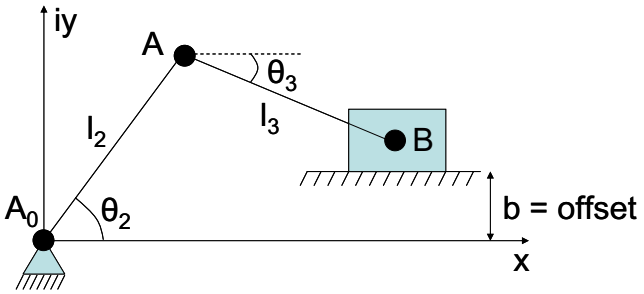

Figure 11.7: Slider-crank mechanism.

11.7.7 *Application of four bar linkage kinematics*

Consider the offset slider crank mechanism shown in Fig. 11.7:

$$\boldsymbol{l_B} = l_2 e^{i\theta_2} + l_3 e^{i(2\pi-\theta_3)} = x + ib \tag{11.95}$$

, and so

$$\dot{\boldsymbol{l}}_{\boldsymbol{B}} = l_2 e^{i\theta_2}(i\dot{\theta}_2) - l_3(i\dot{\theta}_3)e^{i(2\pi-\theta_3)} = \dot{x} \tag{11.96}$$

, where

$$\ddot{\boldsymbol{l}}_{\boldsymbol{B}} = -l_2\dot{\theta}_2^2 e^{i\theta_2} + l_2 i\ddot{\theta}_2 e^{i\theta_2} - l_3\dot{\theta}_3^2 e^{i(2\pi-\theta_3)} - l_3 i\ddot{\theta}_3 e^{i(2\pi-\theta_3)} = \ddot{x}. \tag{11.97}$$

The unknowns are $\dot{\theta}_3$, $\ddot{\theta}_3$, $\dot{x}$ and $\ddot{x}$. The x and y components for the position are given by

$$l_2(\cos\theta_2 + i\sin\theta_2) + l_3(\cos\theta_3 - i\sin\theta_3) = x + ib; \tag{11.98}$$

rewriting,

$$l_2\cos\theta_2 + l_3\cos\theta_3 = x \tag{11.99}$$

and

$$l_2\sin\theta_2 - l_3\sin\theta_3 = b. \tag{11.100}$$

Once x is known, $\dot{\theta}_3$ and $\dot{x}$ can be determined:

$$i\dot{\theta}_2 l_2(\cos\theta_2 + i\sin\theta_2)' - i\dot{\theta}_3 l_3(\cos\theta_3 - i\sin\theta_3) = \dot{x} \tag{11.101}$$

$$-\dot{\theta}_2 l_2 \sin\theta_2 - l_3\dot{\theta}_3 \sin\theta_3 = \dot{x} \tag{11.102}$$

$$\dot{\theta}_2 l_2 \cos\theta_2 - l_3\dot{\theta}_3 \cos\theta_3 = 0 \tag{11.103}$$

Finally, $\ddot{x}$ and $\ddot{\theta}_3$ are calculated.

Figure 11.8: Four-bar linkage: full suspension in a mountain bike.

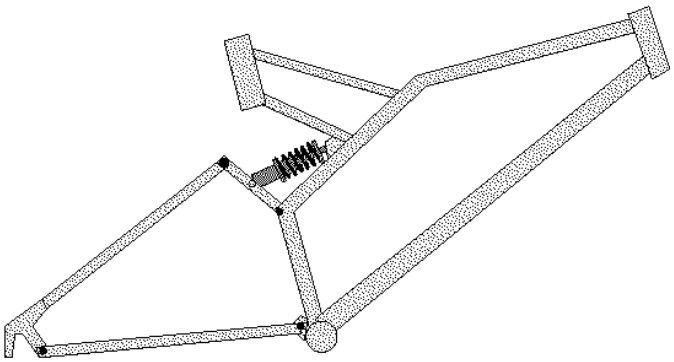

Figure 11.9: Mountain bike suspension schematic.

Example 11.7.1. Mountain bikes these days exist in so-called "full suspension" configurations, as shown in Fig. 11.8. The rear suspension is usually driven by a four bar linkage. Figure 11.9 shows a schematic of a full suspension bike frame. The dimensions and angles are indicated in Fig. 11.10.

The box $ABCD$ represents the four bar linkage (rocker-rocker type). The four bar linkage is mounted (fixed) to the rest of the frame in points A and B. The rear wheel shaft is mounted in point D. A Cartesian coordinate system has been defined in the figure; h represents the

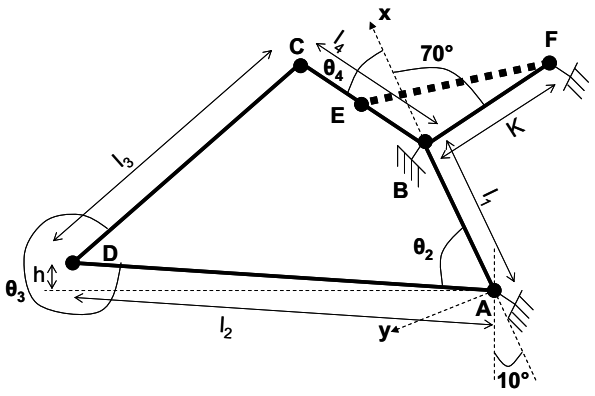

Figure 11.10: Mountain bike suspension detail.

height of the rear wheel above the horizontal help-line, starting from point A. The initial value for $\theta_2 = 65°$. The dimensions of the bars are $l_1 = 0.3$ m, $l_2 = 0.4$ m, $l_3 = 0.3$ m, $l_4 = 0.2$ m. The length of the crank is $K = 0.2$ m, the line EF represents the damper. The distance $|CE| = |EB|$, i.e., the damper is mounted in the middle of bar l_4.

1. Calculate h in the initial configuration. We can calculate the angle β between the horizontal helpline and the bar l_2 as $90° - (65° + 10°) = 15°$. Thus, $h_{\text{init}} = l_2 \times \sin\beta$. Hence, $h_{\text{init}} = 0.1035$ m.

2. Assume a mountain biker using this frame rides over a cobblestone, a semi-circular bump (2D), as shown in Fig. 11.11, with a velocity of 30 km/h. Assume the rear wheel keeps continuous contact with the bump. (Note: this assumption is not correct in a real situation but simplifies the problem) Plot the angle θ_4 versus time, as the

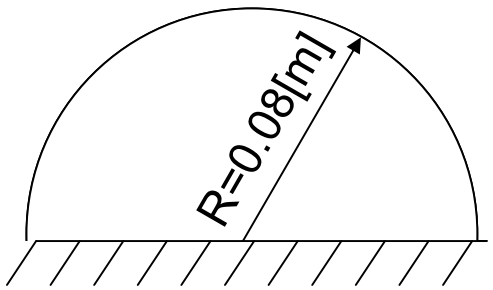

Figure 11.11: Cobblestone model.

mountain biker rides over the bump with his rear (fully suspended) wheel. Assume the tires are infinitely stiff and the rear wheel shaft remains vertical above the contact point between the rear wheel and the contour of the bump, i.e., the vertical displacement of the bump is directly transferred to point D and superposed with the initial value for h.

3. By determining the y-displacement of the half circular bump and superposing them with h_{init}, we find the total vertical displacement at point D. Since the velocity of the biker is known, it can be calculated how long it takes to ride over the bump. $2 \times \pi \times r_{\text{bump}} = 0.25$ m. At 30 km/h or 8.33 m/s, it takes 0.03 s to overcome the bump. Know we can calculate the step size of our time grid with 180 nodes: 1.67×10^{-4} s. Knowing the time grid, we can create a time vector in Matlab, which can be used to plot the angle. Since we know the total vertical displacement at point D in time, we can calculate β in time and thus θ_2 in time. The plot of $\theta_2(t)$ looks as shown in Fig. 11.12.

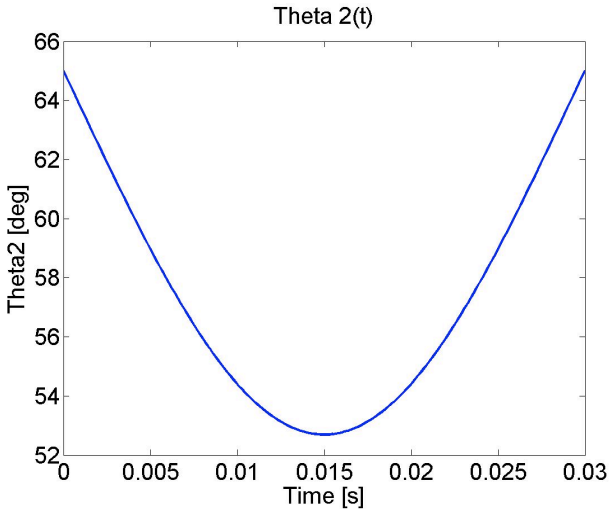

Figure 11.12: Angle θ_2 versus time.

4. Now we solve the four bar linkage at every time step with the iterative method to find $\theta_4(t)$. The plot of $\theta_4(t)$ looks is shown in Fig. 11.13.

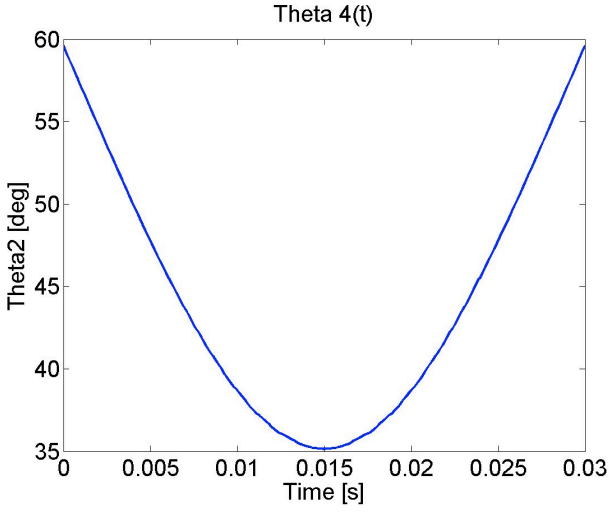

Figure 11.13: Angle θ_4 versus time.

5. We know the damper is attached in the middle of crank CB. Calculate the maximum 'compression way' the damper undergoes by hitting the bump. After determining $\theta_4(t)$, we know the maximum value and minimum value for θ_4. Together with the given angle of 70°, we can calculate the length $|EF|$, in the triangle EFB. The maximum $\theta_4 = 1.0402$ rad and the minimum $\theta_4 = 0.61353$ rad.

6. We calculate the length $|EF|$, once for the triangle EFB with maximum θ_4 and once for triangle EFB with minimum θ_4. The difference between both lengths gives the maximum compression of the damper = 0.02889 m.

11.7.8 *Precision point analysis*

If one desires that the output lever of a four bar mechanism occupies the specific positions ϕ_1, ϕ_2, ϕ_3, corresponding to angular positions ψ_1, ψ_2, ψ_3 of the input lever, the following approach can be followed. From Freudenstein's equation one finds that

$$L_3 - \cos(\theta_2 - \theta_4) + L_2 \cos\theta_4 - L_1 \cos\theta_2 = 0. \tag{11.104}$$

Replacing θ_2 with ψ_1, ψ_2, ψ_3, respectively, and doing the same for θ_4 by replacing it with ϕ_1, ϕ_2, ϕ_3 gives

$$L_3 + L_2 \cos\phi_1 - L_1 \cos\psi_1 = \cos(\psi_1 - \phi_1) \tag{11.105}$$

$$L_3 + L_2 \cos\phi_2 - L_1 \cos\psi_2 = \cos(\psi_2 - \phi_2) \tag{11.106}$$

$$L_3 + L_2 \cos\phi_3 - L_1 \cos\psi_3 = \cos(\psi_3 - \phi_3). \tag{11.107}$$

Solving eqns. (11.105), (11.106) and (11.107) simultaneously gives L_1, L_2 and L_3.

Example 11.7.2. Assume that one wants to synthesize the equation $y = 1/x$ using three precision points. It is specified that $x_1 = 1.067$, $x_2 = 1.5$ and $x_3 = 1.933$. From $y = 1/x$ one finds that $y_1 = 0.937$, $y_2 = 0.667$ and $y_3 = 0.517$, respectively. The following specifications apply: 30 degree input angle and 90 degree total swing for the input lever and 240 degrees and 90 degree total travel for the output lever. Now interpolate the angles between $x = 1$ and $x = 2$ and $y = 1$ and $y = 0.5$

$$-L_1 \cos(36.03) + L_2 \cos(251.34) + L_3 = \cos(36.03 - 71.34) \tag{11.108}$$

$$-L_1 \cos(75) + L_2 \cos(300) + L_3 = \cos(75 - 120) \tag{11.109}$$

$$-L_1\cos(113.97)+L_2\cos(326.94)+L_3=\cos(113.97-146.94) \quad (11.110)$$

This becomes

$$L_1 = 0.4032 \quad (11.111)$$

$$L_2 = 0.4032 \quad (11.112)$$

$$L_3 = 1.0130 \quad (11.113)$$

Using $l_1 = 1$

$$l_4 = \frac{l_1}{L_1} = 2.48 \quad (11.114)$$

$$l_2 = \frac{l_1}{L_2} = 2.48 \quad (11.115)$$

11.8 *Graph theory, incidence matrices, and multiple rigid body dynamics*

11.8.1 *Introduction to graph theory terminology*

We've talked about connected bodies with joints like those in Fig. 11.14 (from Moon[1]), and we now note that most such systems we have looked at have been *closed chains*—where the connected objects do not have a free end, like Fig. 11.15(b) (from Moon[2]). Robotic arms are typically *open chains*—the end (where the *effector* is at) in Fig. 11.15(a) is free to move based upon the motion of the objects that connect to reach that end from a mounting. Most systems are really a combination of both open and closed chains, like Fig. 11.15(c). Here, we follow generally the approach of Moon[3],[4] and refer the reader to that text for far more comprehensive treatment of the topic.

Recalling the equations of dynamics (or motion) for single rigid bodies,

$$\sum \boldsymbol{F} = \frac{d}{dt}(m\dot{\boldsymbol{r}}) \quad \text{and} \quad \sum \boldsymbol{T} = \frac{d}{dt}\boldsymbol{H} = \boldsymbol{I}\cdot\dot{\boldsymbol{\omega}} \quad (11.116)$$

where $\boldsymbol{\omega} = \omega_1\hat{\boldsymbol{e}}_1 + \omega_2\hat{\boldsymbol{e}}_2 + \omega_3\hat{\boldsymbol{e}}_3$ using body-based coordinates, for example.

For more than one body, we need to treat the interconnection between the bodies (*see* Grübler's equation, eqn. (11.1), for example), and the transmission of forces and moments as a consequence. We have seen some of this with four bar linkages and classic methods of expressing the kinematics, but now we make an introduction into

[1] Francis C Moon. *Applied dynamics: with applications to multibody and mechatronic systems*. John Wiley & Sons, 2008

[2] Francis C Moon. *Applied dynamics: with applications to multibody and mechatronic systems*. John Wiley & Sons, 2008

[3] Francis C Moon. *Applied dynamics: with applications to multibody and mechatronic systems*. John Wiley & Sons, 2008

[4] Worth noting that Moon's derivations in his text are incorrect in the details—be careful.
Francis C Moon. *Applied dynamics: with applications to multibody and mechatronic systems*. John Wiley & Sons, 2008

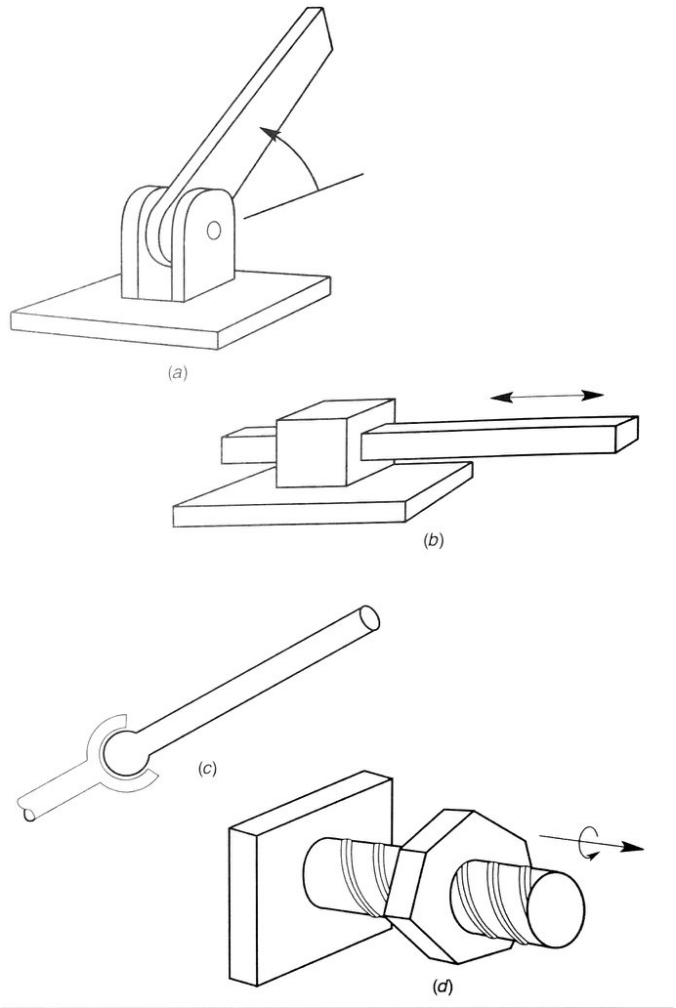

Figure 11.14: Different types of joints: (a) pinned, (b) prismatic, (c) revolute, (d) threaded.

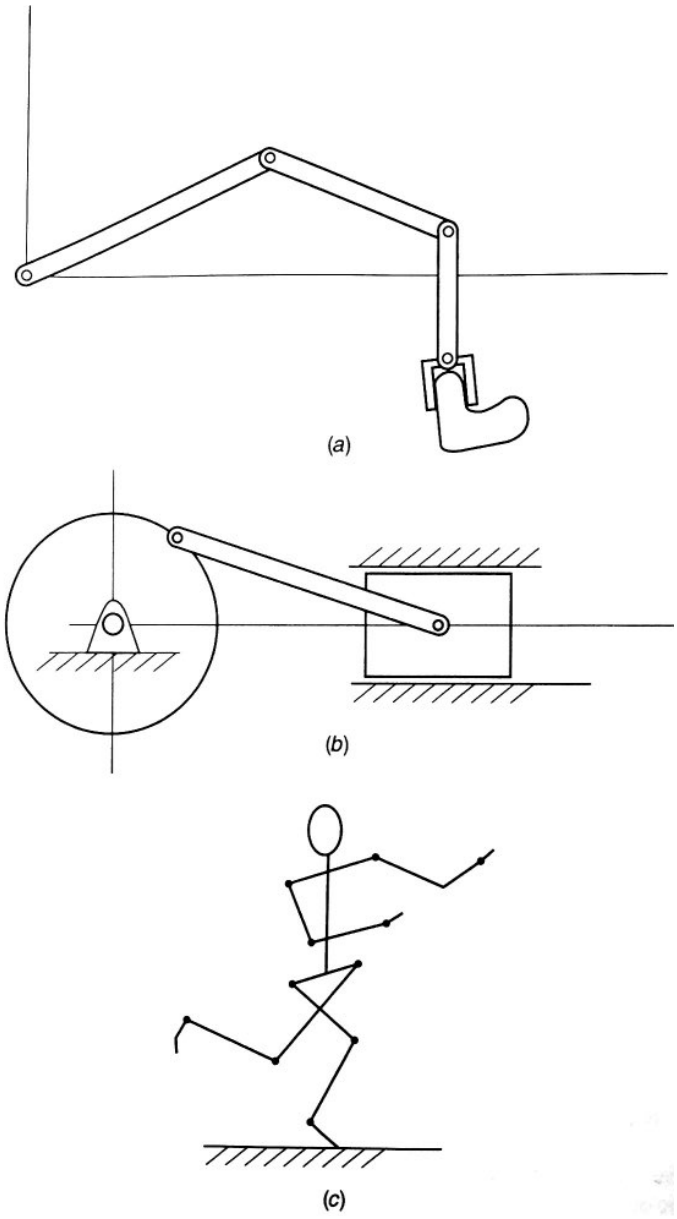

Figure 11.15: Types of rigid body groupings: (a) open chain, (b) closed chain, and (c) a mixture of both.

a slightly more involved approach, using *graph theory* and *incidence matrices*.

We can represent the interconnections between n bodies of a mechanism by a graph, for example as shown in Fig. 11.16 (from Moon[5]) The n bodies S_i are connected by m joints u_j; in graph theory

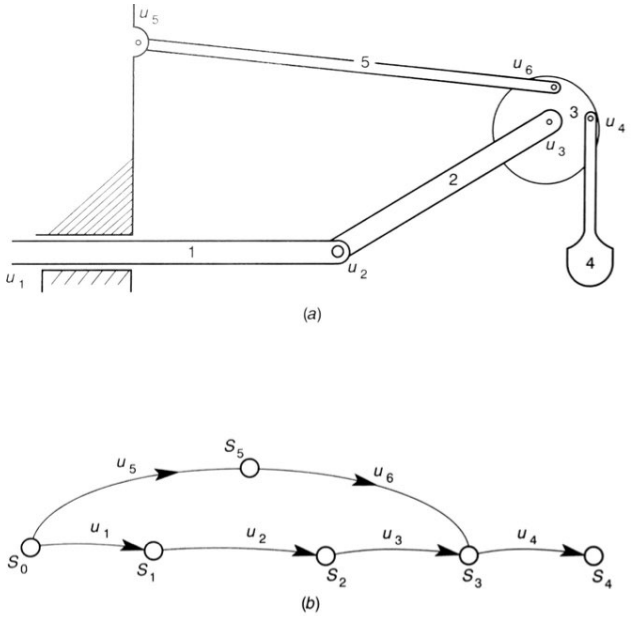

[5] Francis C Moon. *Applied dynamics: with applications to multibody and mechatronic systems*. John Wiley & Sons, 2008

Figure 11.16: A mechanism composed of (a) rigid bodies and its (b) graph theory-based representation.

these terms are defined as *vertices* S_i and *edges* u_j, respectively. Notice the zeroth body/vertex S_0: this is the mounting or the base, and is important to include in the model. *The number of joints m in a mechanism must be equal or one fewer than the number of bodies n, taking into account the zeroth body if it exists, and making sure to count the joint at the intersection of more than two bodies as more than one joint.* For example, three bars with a shared joint represent *two joints*: one for each pair of bars. The direction of the arrows as shown is arbitrary. Notice the paths along the graph, from S_0 to S_n, for example, via the joints/edges $u_1, u_2, \ldots, u_m$. An edge u_j is *incident* with S_k and S_l if it connects these two bodies/vertices. We then can define the *incidence matrix* $[S]$ (of rows i: bodies and columns j: joints) formed with elements of value $-1, 0$, or $+1$—*only*—helping to indicate how the vertices/bodies are connected through the edges/joints:

$$S_{ij} = \begin{cases} +1 & \text{if edge } u_j \text{ is directed } \textit{away} \text{ from } S_i \\ -1 & \text{if edge } u_j \text{ is directed } \textit{toward} \text{ from } S_i \\ 0 & \text{if edge } u_j \text{ is not incident (not connected) to } S_i \end{cases} \tag{11.117}$$

If $[S]$ *is* a square $n \times m$ matrix where $m = n$, then we define $[\mathbb{S}] = [S]$. If $[S]$ is *not* a square $n \times m$ matrix where $m = n$, then it must be that

$m = n - 1$ and the matrix $[S]$ may be written as a row vector $\left[S_{0j}\right]$ augmented to an $n \times n$ matrix $[\mathbb{S}]$:

$$[S] = \begin{bmatrix} \left[S_{0j}\right] \\ [\mathbb{S}] \end{bmatrix}. \tag{11.118}$$

Regardless, the matrix $[\mathbb{S}]$ can be shown to have an inverse $[\mathbb{T}] = [\mathbb{S}]^{-1}$ and $[\mathbb{T}]^T \left[S_{0j}\right]^T = [-\mathbb{1}]$, which is an $n \times 1$ column matrix of -1 entries. Now

$$T_{ji} = \begin{cases} +1 & \text{if edge } u_j \text{ lies along the path } S_0 \text{ to } S_i \text{ and points } \textit{toward } S_0 \\ -1 & \text{if edge } u_j \text{ lies along the path } S_0 \text{ to } S_i \text{ and points } \textit{away} \text{ from } S_0 \\ 0 & \text{if edge } u_j \text{ is not along the path } S_0 \text{ to } S_i. \end{cases} \tag{11.119}$$

An example helps.

Example 11.8.1. Robot arm.

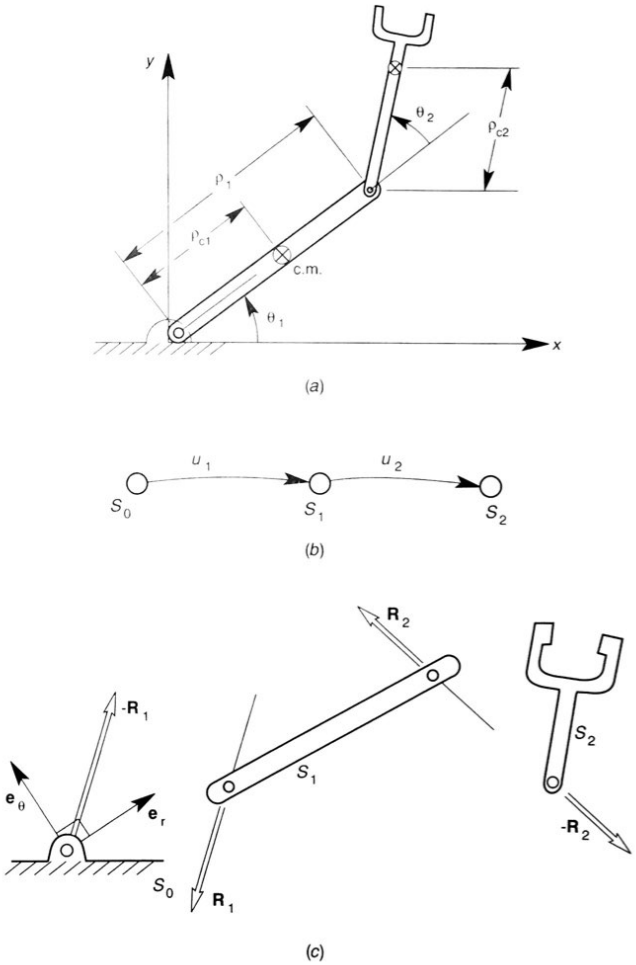

Figure 11.17: (a) A robot arm, (b) its graph representation, and (c) the reaction forces arising at the joints.

Remember that i refers to the rigid bodies and j to the joints between them. The connection graph (from Moon[6]) is shown in Fig. 11.17(b)

from the robot arm in Fig. 11.17(a). So

$$[S] = \begin{bmatrix} S_{01} & S_{02} \\ S_{11} & S_{12} \\ S_{21} & S_{22} \end{bmatrix}, \tag{11.120}$$

where we can determine the values of each of these terms using eqn. (11.117):

$$\begin{aligned} S_0 : &\begin{cases} u_1 \text{ connected, away} \implies & S_{01} = +1 \\ u_2 \text{ not connected} \implies & S_{02} = 0 \end{cases} \\ S_1 : &\begin{cases} u_1 \text{ connected, toward} \implies & S_{11} = -1 \\ u_2 \text{ connected, away} \implies & S_{12} = +1 \end{cases} \\ S_2 : &\begin{cases} u_1 \text{ not connected} \implies & S_{21} = 0 \\ u_2 \text{ connected, toward} \implies & S_{22} = -1 \end{cases} \end{aligned} \tag{11.121}$$

and so

$$[S] = \begin{bmatrix} 1 & 0 \\ -1 & 1 \\ 0 & -1 \end{bmatrix}. \tag{11.122}$$

Example 11.8.2. More complex system from Fig. 11.16

This more complex version is composed of $n = 6$ bodies $i \in \{0, 1, \ldots, 5\}$, including the base, and altogether six joints, $j \in \{1, \ldots, 6\}$, producing a 6×6 matrix:

$$\begin{bmatrix} S_{01} & S_{02} & S_{03} & S_{04} & S_{05} & S_{06} \\ S_{11} & S_{12} & S_{13} & S_{14} & S_{15} & S_{16} \\ S_{21} & S_{22} & S_{23} & S_{24} & S_{25} & S_{26} \\ S_{31} & S_{32} & S_{33} & S_{34} & S_{35} & S_{36} \\ S_{41} & S_{42} & S_{43} & S_{44} & S_{45} & S_{46} \\ S_{51} & S_{52} & S_{53} & S_{54} & S_{55} & S_{56} \end{bmatrix}. \tag{11.123}$$

The first row ends up being $[+1\ 0\ 0\ 0\ +1\ 0]$.

11.8.2 *Equations of motion from graph theory*

Why do we bother with graph theory? Because this helps us write the complete set of equations of motion for the system and can be regularized to run on a computer.

We consider only one of the bodies S_i making up the robot arm, for example, as shown in Fig. 11.17. There are forces of constraint $\boldsymbol{R}_1$ and $\boldsymbol{R}_2$ at the left and right joints, and hinge moments—or *couples*—$\boldsymbol{C}_1$ and $\boldsymbol{C}_2$ that arise as well. These are about the center of mass, denoted `c.m.` in the figure. These forces may arise from the adjacent members, but there may also be joint friction, springs, or dampers involved to contribute to $\boldsymbol{C}_1$ and $\boldsymbol{C}_2$.

We choose a sign convention such that $\boldsymbol{R}_j$ is positive the direction of positive u_j. If u_j is toward S_i and away from S_k, then $\boldsymbol{R}_j$ is positive if and only if it is toward S_i and away from S_k.

The equations of motion for the force may then be written as

$$\frac{d}{dt}\left(m_i\dot{\boldsymbol{r}}_i\right) = \boldsymbol{F}_i^A + S_{ij}\boldsymbol{R}_j + S_{ik}\boldsymbol{R}_k. \tag{11.124}$$

In general, for m joints and n bodies,

$$\frac{d}{dt}\left(m_i\dot{\boldsymbol{r}}_i\right) = \boldsymbol{F}_i^A + \sum_{j=1}^{m} S_{ij}\boldsymbol{R}_j \tag{11.125}$$

for $i \in \{1,\dots,n\}$. For the *angular* equations of motion that we will also require, we need the moment arms $\boldsymbol{\rho}_{i1}$ and $\boldsymbol{\rho}_{i2}$ as shown in the figure, from the center of mass to the two joints;

$$\dot{\boldsymbol{H}}_i = \boldsymbol{M}_i^A + \sum_{j=1}^{m} S_{ij}\left(\boldsymbol{\rho}_{ij}\times\boldsymbol{R}_j + \boldsymbol{C}_j\right), \tag{11.126}$$

where $\boldsymbol{M}_i^A$ is the applied moment about the center of mass (using the parallel axis theorem to accomplish this as needed).

Turns out we can rearrange the equation of motion to find the constraint forces, if we know the dynamics—and we need that $[\mathbb{T}]$ to do so:

$$\boldsymbol{R}_j = \sum_{i=1}^{n} T_{ji}\left[\frac{d}{dt}\left(m_i\dot{\boldsymbol{r}}_i\right) - \boldsymbol{F}_i^A\right]. \tag{11.127}$$

Example 11.8.3. Robot arm dynamics from Fig. 11.17

We try all this out with an example, finding the equations of motion for the robot arm in Fig. 11.17. Assuming there are no joint moments $\boldsymbol{C}_j$ nor body moments $\boldsymbol{M}_i^A$ being applied, the equations of motion are

$$\begin{aligned}
m_1\ddot{\boldsymbol{r}}_1 &= -m_1 g\boldsymbol{e}_y + \sum_{j=1}^{2} S_{1j}\boldsymbol{R}_j \\
m_2\ddot{\boldsymbol{r}}_2 &= -m_2 g\boldsymbol{e}_y + \sum_{j=1}^{2} S_{2j}\boldsymbol{R}_j \\
I_1\dot{\boldsymbol{\omega}} &= \boldsymbol{e}_z\cdot\sum_{j=1}^{2} S_{1j}\left(\boldsymbol{\rho}_{1j}\boldsymbol{R}_j\right) \\
I_2\dot{\boldsymbol{\omega}} &= \boldsymbol{e}_z\cdot\sum_{j=1}^{2} S_{2j}\left(\boldsymbol{\rho}_{2j}\boldsymbol{R}_j\right)
\end{aligned} \tag{11.128}$$

for the two bodies. Naturally we don't have to worry about the zeroth body: the mounting itself. Solving these as a system would give the motion of the robotic arm. Notice how determination of the values of S_{ij} defines the relationship between the equations of motion in concert with how the objects are actually connected together.

11.8.3 *Graph theory applies to far more than mechanical problems*

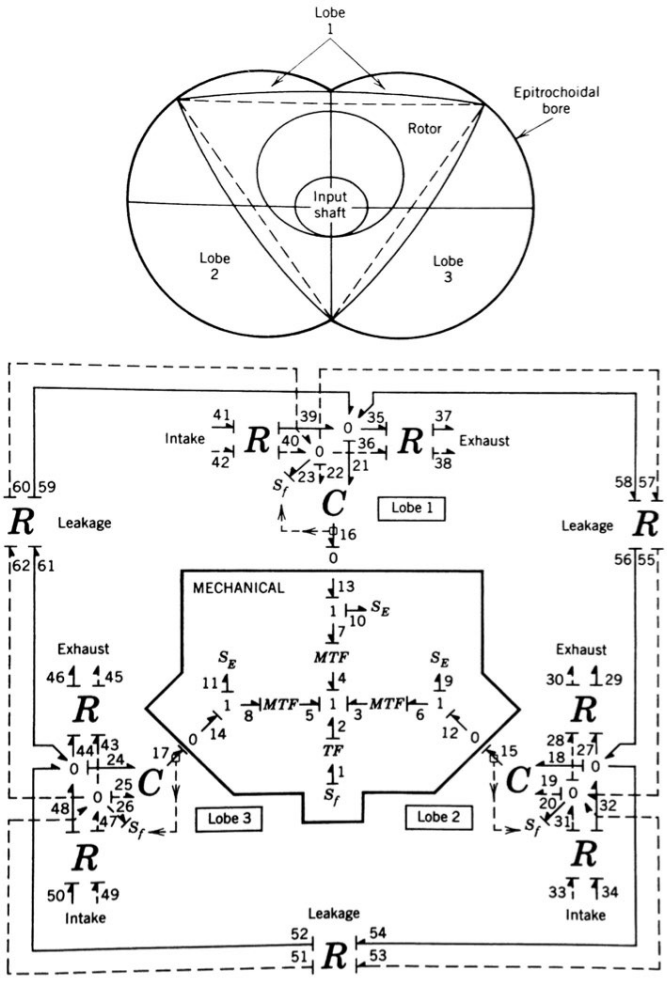

Figure 11.18: (a) A graph theoretic representation of a Wankel engine, including the thermodynamics and physical dynamics.

Worth noting—finally—that graph theory extends to far more general problems, and well beyond mechanical engineering and structural analysis; Fig. 11.18 (from Karnopp, et al.[7]) illustrates how advanced such techniques can become, and a proficient user of the methods described in graph theory can analyze extremely complex problems in a consistent, coherent fashion.

[7] Dean C Karnopp, Donald L Margolis, and Ronald C Rosenberg. *System dynamics: a unified approach*. John Wiley, third edition, 1990